SCIENCE CHINA Materials ARTICLES

mater.scichina.com link.springer.com

Published online 29 March 2019 | https://doi.org/10.1007/s40843-019-9417-5
Sci China Mater 2019, 62(8): 1177–1187

Graphene oxide quantum dots embedded polysulfone membranes with enhanced hydrophilicity, permeability and antifouling performance

Guoke Zhao, Ruirui Hu, Jing Li and Hongwei Zhu*

ABSTRACT Graphene oxide (GO) has been demonstrated to be an effective hydrophilic nanofiller to modify the polymeric membranes when forming a mixed matrix structure. GO quantum dots (QDs) are promising candidates to fully exert the rich oxygen containing functional groups due to their unique size induced edge effects. In this work, GO QDs modified polysulfone (PSF) ultrafiltration (UF) membranes were prepared by phase inversion method with various GO QDs loadings (0.1–0.5 wt.%). A proper amount of GO QDs addition led to a more porous and hydrophilic membrane structure. With 0.3 wt.% GO QDs, the membranes showed a 60% increase in permeability (130.54 *vs.* 82.52 LMH bar^{-1}). The pristine PSF membranes had a complete cutoff of bovine serum albumin molecules and it was well maintained with GO QDs incorporated. The membranes with 0.5 wt.% GO QDs exhibited the highest flux recovery ratio of 89.7% and the lowest irreversible fouling of 10.3% (54.5% and 33.3% for the pristine PSF membranes). Our results proved that GO QDs can function as effective nanofillers to enhance the hydrophilicity, permeability and antifouling performance of PSF UF membranes.

Keywords: graphene oxide, quantum dots, ultrafiltration membrane, antifouling

Introduction

Contaminants released into the environment are of big threat to human health and the ecological system, thus the purification of waste water deserves special attention [1–3]. Ultrafiltration (UF) is widely used for water purification due to its high efficiency, cost effectiveness, simple operation and zero production of harmful by-products. Hence, UF membranes are heavily utilized in separation processes in the food, pharmaceutical and paper processing industries [4,5]. Polysulfone (PSF) is a commonly used polymeric UF membrane material due to its desirable mechanical, thermal and chemical stability [6]. However, the inherent hydrophobic characteristic of PSF leads to severe membrane fouling, during which the water transport resistance increases due to pore narrowing, pore blocking and cake layer formation. The membrane flux decreases significantly with the operation time, leading to increased energy demand and operational costs [7–9]. Therefore, effective mitigation of membrane fouling is a key research area in UF technologies.

The fouling resistance of UF membranes is mainly influenced by their surface properties, including hydrophilicity, roughness and surface charge. A hydrophilic and smooth surface can effectively hinder foulant accumulation and deposition, thus relieving membrane fouling [10,11]. Various approaches have been proposed to ameliorate the fouling tendency of polymeric membranes through modifying their surface properties (mostly hydrophilicity), including surface coating [12], plasma treatment [13], chemical modification [14] and blending with hydrophilic fillers [15]. Incorporation of inorganic nanoparticles (NPs) into the membrane matrix has been proven to be a straightforward and effective method to modify the pore structure and surface properties of the nanocomposite membranes. The employed inorganic NPs are generally hydrophilic, such as TiO_2 [16], SiO_2 [17], Al_2O_3 [18], ZrO_2 [19] and Fe_3O_4 [20]. NPs influence the pore forming process and the hydrophilicity of the membranes so that water flux, rejection, thermo-mechanical stability and antifouling performance of the membranes are improved. However, a high weight percentage of NPs is required to obtain noticeable effects and in addition, it is hard for these NPs to be uniformly dispersed in the casting solutions [21].

Recently, graphene oxide (GO) has become a promising

State Key Lab of New Ceramics and Fine Processing, School of Materials Science and Engineering, Tsinghua University, Beijing 100084, China
* Corresponding author (email: hongweizhu@tsinghua.edu.cn)

membrane material owing to its impressive separation performance [22–25]. GO membranes possess ultrafast water transport properties and extraordinary water adsorption characteristics [26,27]. GO sheets have also been proven to be effective nanofillers to improve the overall performance of polymeric UF membranes, due to their high aspect ratio, low density, easy functionalization and abundance of oxygen containing functional groups [28–30]. Blending GO sheets into PSF UF membrane matrix will greatly improve the membrane hydrophilicity, which further enhances water affinity to the membrane surfaces and the drag force for water transportation, leading to increased water flux. Furthermore, a hydration layer can be formed on a hydrophilic membrane surface which hinders the adsorption of foulants, resulting in improved antifouling performance [31,32]. However, the effective oxygen containing functional groups are located at the edges and defective regions of the GO sheets. The basal plane is mainly composed of sp^2 carbon atoms. It is desirable for more hydrophilic functional groups to be distributed at membrane surfaces. However, GO sheets tend to aggregate and form non-homogeneous distributions when large quantities are incorporated. The agglomeration of GO sheets results in defects and a decrease in membrane hydrophilicity and solute rejection [33,34]. It is highly desirable that GO sheets possess more edges in order to improve membrane hydrophilicity and performance.

GO quantum dots (QDs) are nanometer-sized fragments of GO sheets, with a lateral size smaller than 100 nm. They share the same structure as GO sheets yet the amount of functional groups is higher due to edge effects [35,36]. GO QDs have been employed as nanofillers to modify thin film composites in nanofiltration, reverse osmosis, forward osmosis and pervaporation dehydration membranes during the interfacial polymerization process. The modified mixed matrix membranes showed enhanced permeability, antifouling and chlorine resistance [37–41]. It is expected that GO QDs can increase the hydrophilicity, permeability and fouling resistance of PSF UF membranes more effectively comparing with GO sheets.

In the present work, GO QDs were incorporated into PSF UF membrane matrix during the phase inversion process to form GO QDs/PSF hybrid membranes. These membranes were characterized in terms of morphology, pore structure, surface roughness, porosity and water contact angle. The effects of GO QDs on the permeability and antifouling performance of the hybrid membranes and the underlying mechanisms were investigated in detail.

As illustrated in Fig. 1, the mixture dispersion of GO QDs/PSF/1-methyl-2-pyrrolidinone (NMP) was prepared and then cast on a glass plate. GO QDs migrated to membrane surfaces and pore walls spontaneously during the phase inversion process [42]. The improved hydrophilicity mitigated membrane fouling by reducing the adhesion force between membrane surfaces and foulant proteins. Furthermore, a hydration layer was formed on the GO QDs modified membrane surfaces, which also hindered protein adsorption. As a result, membrane fouling resistance was greatly improved by the incorporation of GO QDs into the membrane matrix. The enhanced membrane hydrophilicity was also beneficial for the improvement of membrane flux, because more water molecules could be attracted to the membrane surfaces. In addition, the incorporation of GO QDs led to a more porous membrane structure, which reduced the resistance to water transportation.

EXPERIMENTAL SECTION

Materials

PSF granules were purchased from Sigma-Aldrich Chemical Co., Ltd (China). The solvent NMP was purchased from Aladdin Co., Ltd (China). GO QDs were obtained from Nanjing XFNANO Materials Tech Co., Ltd (China). Bovine serum albumin (BSA) and fluorescein isothiocyanate-BSA (FITC-BSA) were obtained from Beijing Bainuowei Biotechnology Co., Ltd (China) and used to

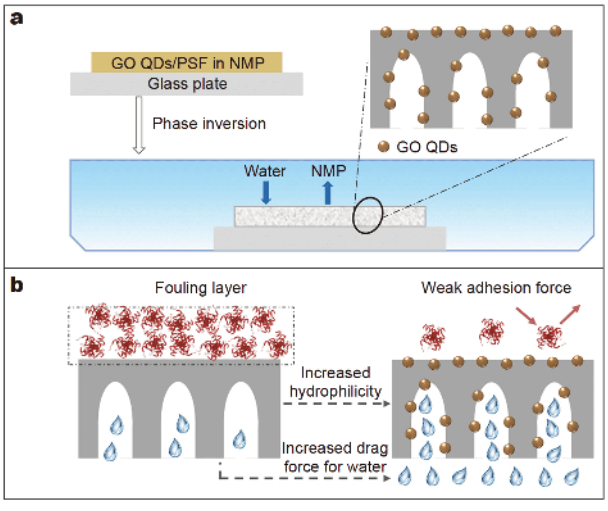

Figure 1 (a) Schematic illustration of the fabrication process of GO QDs/PSF membranes. (b) Diagram of the mechanisms for the improved membrane permeability and fouling resistance.

assess the separation performance of the membranes and the adhesion force between typical proteins and the membrane surfaces, respectively. All chemicals were of analytical grade and used without further purification.

Membrane preparation

All membranes were prepared by a common phase inversion method, as shown in Fig. 1. To prepare the casting solutions, a certain quantity of GO QDs were firstly dispersed in 17 g NMP with the assistance of ultrasonication for 2 h. 15 wt.% of PSF (3 g) was then dissolved into the uniformly dispersed GO QDs suspension stirring overnight to obtain a homogeneous casting solution. The mass percentage of GO QDs in the casting solutions was 0, 0.1%, 0.3% and 0.5%, with respect to the weight of PSF. The membranes were denoted as PSF membranes, QDs-0.1, QDs-0.3 and QDs-0.5, respectively. Before casting, the solutions were fully degassed in a vacuum oven at 50°C for 6 h. Membranes were then cast on a glass plate using a casting knife with a thickness of 150 μm. The wet membranes with the underlying glass plate were then transferred into the water coagulation bath immediately at room temperature. The fabricated membranes were peeled off from the glass plate after approximately 10 min and transferred to a fresh water bath for storage.

Characterization of GO QDs and the casting solutions

The morphology of GO QDs was studied using transmission electron microscopy (TEM, JEM-2100F, JEOL, Japan). TEM samples were prepared by dropping the well dispersed GO QDs water suspension onto carbon coated copper grids, and then fully dried in vacuum at room temperature. Chemical composition of GO QDs was confirmed by X-ray photoelectron spectroscopy (XPS, ESCALAB 250Xi, Thermo Fisher, USA). The viscosity of the casting solutions was measured by a rheometer (MCR302, Anton Paar, Austria). Data was acquired in the shear rate range of 10–100 s^{-1} at 20°C.

Characterization of the membranes

To investigate the effects of GO QDs on the pore structure of the membranes, scanning electron microscopy (SEM, MERLIN Compact, ZEISS, Germany) was used to characterize the surface and cross-sectional morphologies of the membranes. The SEM surface samples were directly cut from the dried membranes and stuck onto a copper substrate with conductive plastic. For the cross-sectional samples, dried membranes were fractured with liquid nitrogen. All the samples were sputter-coated with 5 nm of platinum using ion beam coater (Model 681, Gatan, USA) before observation. Surface roughness of the membranes was studied with atomic force microscopy (AFM, MFP-3D infinity, Oxford, USA). The scanning area was 20 μm×20 μm for each image. The average value of the mean roughness (R_a) was obtained based on at least three scanning locations to quantify the membrane surface roughness. Static water contact angles of the membrane surfaces were measured by a testing system (SPCA, HARKE, China). The dried membranes were fixed onto a glass plate and 4 μL of water was dropped onto the membrane surface with a syringe. A static image was then captured and the contact angle was measured. Five measurements were performed for each sample under the same condition and the average was reported. The membrane porosity ε (%), defined as the ratio of pore volume to the total volume of the porous membrane, was determined by gravimetric method with the equation:

$$\varepsilon = \frac{W_1 - W_2}{A \cdot d \cdot \rho}, \quad (1)$$

where W_1 is the weight of the wet membrane; W_2 is the weight of the fully dried membrane; A is the membrane area; d is the membrane thickness, ρ is the water density (0.998 g cm^{-3}).

Permeation and rejection measurements

The measurements were conducted using a dead-end permeation cell with an effective membrane filtration area of 12.56 cm^2 at room temperature. The testing pressure was provided by nitrogen. The filtrate was weighed automatically by a digital balance connected to a computer. Membranes were pre-compacted with DI water under 0.2 MPa for 2 h to obtain a steady flux before switching to 0.1 MPa for effective measurements. The water flux, J_w (L m^{-2} h^{-1} bar^{-1}, LMH bar^{-1}), was defined as the volume of the filtrate passing through the membrane per area, per time, per transmembrane pressure. It was determined with the following equation:

$$J_w = \frac{V}{A \cdot \Delta T \cdot \Delta P}, \quad (2)$$

where V (L) is the volume of the filtrate, A (m^2) is the effective membrane filtration area, ΔT (h) is the permeation time, ΔP (bar) is the transmembrane pressure.

Afterwards, the feed was switched to BSA solution (500 ppm in phosphate buffer solution (PBS), pH 7.4) to test the separation performance of the membranes. All the tests were conducted with the feed solution stirred at 800 rpm to relieve concentration polarization effects. The rejection (R) was determined with the following equation:

$$R = \frac{C_f - C_p}{C_f} \times 100\%, \quad (3)$$

where C_f is the concentration of the feed solution, C_p is the concentration of the filtrate. These were measured by an ultraviolet-visible spectrophotometer (Hitach UV-2800, Hitach Co., Japan) at the BSA absorption wavelength of 280 nm. For each type of membrane, at least three samples were measured and the average data was reported.

Antifouling performance tests

The antifouling performance test of the membranes can be divided into three time durations. The first 30 min is for the recording of pure water flux (J_0). The following 120 min is for the recording of membrane water flux (J_1) in 500 ppm BSA solution. Afterwards, the membranes were cleaned with DI water in the permeation cell at 400 rpm for 10 min and pure water flux (J_2) was measured again for another 30 min. The membrane water flux with time was plotted to analyze the fouling behavior of the membranes. To quantify the antifouling performance of the membranes, total fouling ratio (R_{total}) was defined as $(J_0-J_1)/J_0\times100\%$, reversible fouling ratio (R_r) as $(J_2-J_1)/J_0\times100\%$, irreversible fouling ratio (R_{ir}) as $(J_0-J_2)/J_0\times100\%$. The flux recovery ratio (FRR) was defined as $J_2/J_0\times100\%$.

Static BSA adsorption performance

The decrease of the adsorption force between proteins and membrane surfaces helps to improve the antifouling performance of the membranes. FITC-BSA was used to investigate the resistance of membrane surfaces to protein adsorption. Square membrane samples with an area of 2 cm×2 cm were immersed into 4 mg L^{-1} FITC-BSA PBS solution for 24 h at room temperature. Afterwards, the samples were taken out, dried and protected from light. They were then fixed onto a glass plate and characterized by confocal laser scanning microscope (CLSM, LSM780, Zeiss, Germany).

RESULTS AND DISCUSSION

Characterization of GO QDs

TEM was employed to characterize the size and morphology of GO QDs (Fig. 2a), which are of near circle morphology and approximately 20 nm in diameter. The elemental mapping result indicated that GO QDs are composed of carbon and oxygen elements, which was further confirmed by XPS (Fig. 2b). The XPS results showed that the amount of functional groups on GO QDs (C/O=1:1) is much higher than that of GO sheets (C/O=2:1). It can be explained by the edge effects of GO QDs, because functional groups tend to locate at edges and defective regions of GO sheets. The deconvolution of the high resolution C 1s spectrum shows three peaks. The one at 284.5 eV corresponds to C–C bonding while the other two at higher binding energies are for C–O bonds (286.6 eV) and C=O bonds (288.4 eV), respectively. The small size of GO QDs facilitates their dispersion in the casting solutions and the abundance of functional groups makes them highly hydrophilic. Both factors contribute to the improvement of membrane hydrophilicity and antifouling performance when introducing GO QDs.

Characterizations of membranes

The viscosity of the casting solutions with different GO QDs loadings are displayed in Fig. 3. It can be seen from Fig. 3a that all the casting solutions are Newtonian fluids as their viscosities are stable in the shear rate range of 1–100 s^{-1}. Introducing 0.1 wt.% GO QDs brought about a small increase in the viscosity. When further increasing the percentage of GO QDs, the viscosity significantly increased. The increased viscosity retarded the exchange between solvent and non-solvent in the phase inversion process, which led to a thicker and denser membrane structure.

The surface and cross-sectional morphologies of the membranes with different GO QDs loadings are shown in Fig. 4. The surfaces are flat with uniformly distributed nano-sized pores. QDs-0.1 and QDs-0.3 membranes have similar surface morphologies as pristine PSF membranes, with a slightly increased pore density. For QDs-0.5 membranes, the number of pores on the surface decreases significantly. Fig. 4b, d, f, h show that all the membranes have a typical asymmetric structure with a thin selective layer on a finger-like porous sub-layer. The dense selective layer plays the active role for separation and the porous sub-layer functions as a mechanical support. The membrane formation process was not altered by the addition of GO QDs. However, there is an obvious change in the microstructure of the sub-layer. For QDs-0.1 and QDs-0.3 membranes, the finger-like micro-voids are wider comparing with those of the pristine PSF membranes, which can be ascribed to the increased speed of mass transfer between NMP and water in the phase inversion process. The thermodynamic instability of the casting solutions was enhanced with the presence of GO QDs, which favored the phase inversion process. The instability of the system led to quicker mixing of the two liquid phases and larger pore channels in the membranes. This is expected to benefit the membrane water perme-

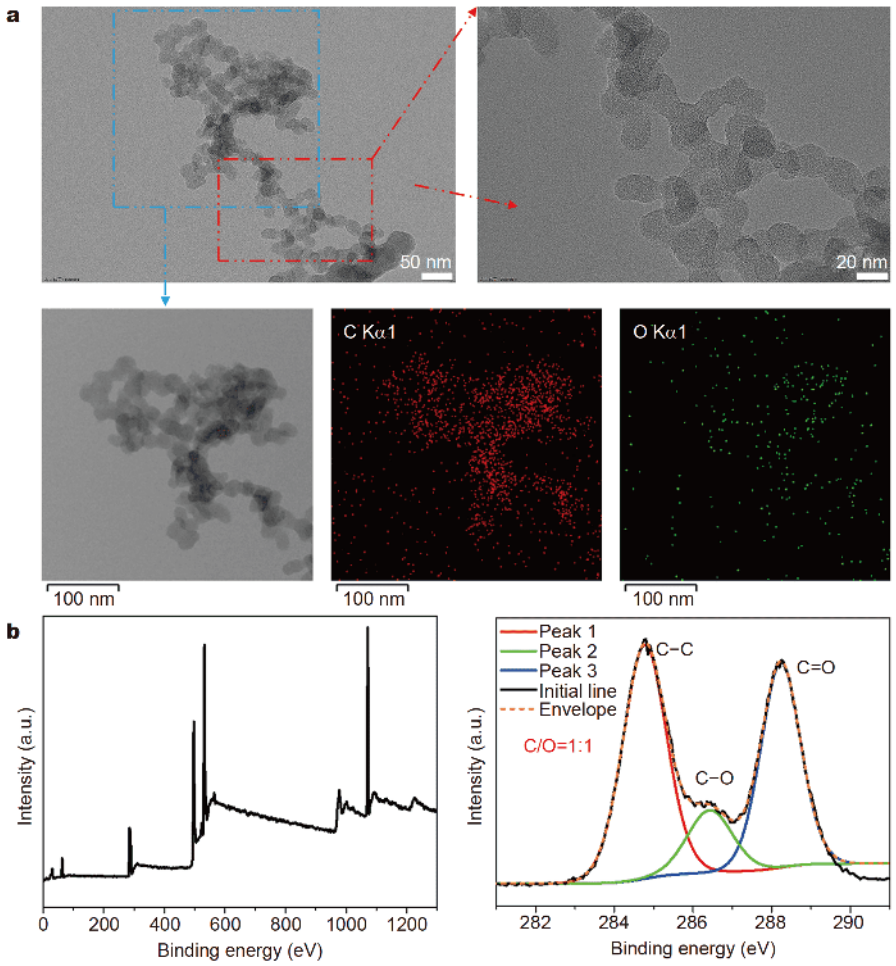

Figure 2 Characterizations of GO QDs. (a) TEM images and elemental mappings; (b) XPS survey and high-resolution C 1s spectra.

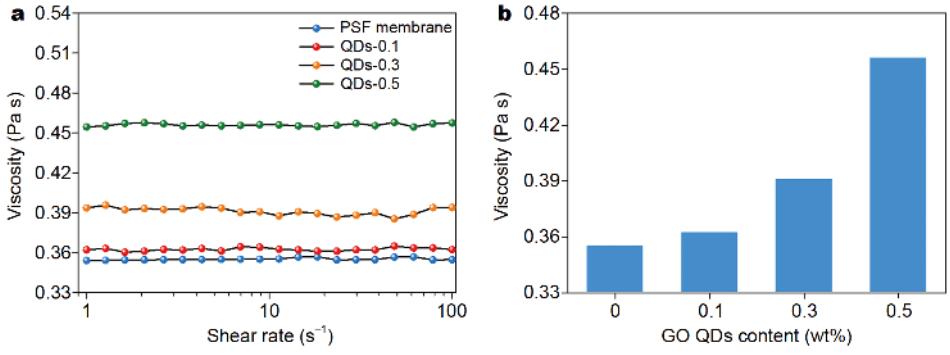

Figure 3 (a) Variation of viscosities of the casting solutions with different GO QDs loadings with shear rate. (b) Comparison of the viscosities of casting solutions with increasing GO QDs loadings.

ability. For QDs-0.5 membranes, the selective layer became denser and the finger-like micro-voids were narrower, which was confirmed by the higher magnification cross-sectional SEM images (Fig. S1). This can be explained by the increased viscosity of the casting solution, which hindered the mixing of NMP and water in the reaction process. When adding a small amount of GO QDs (0.1 wt.% and 0.3 wt.%) into the casting solutions,

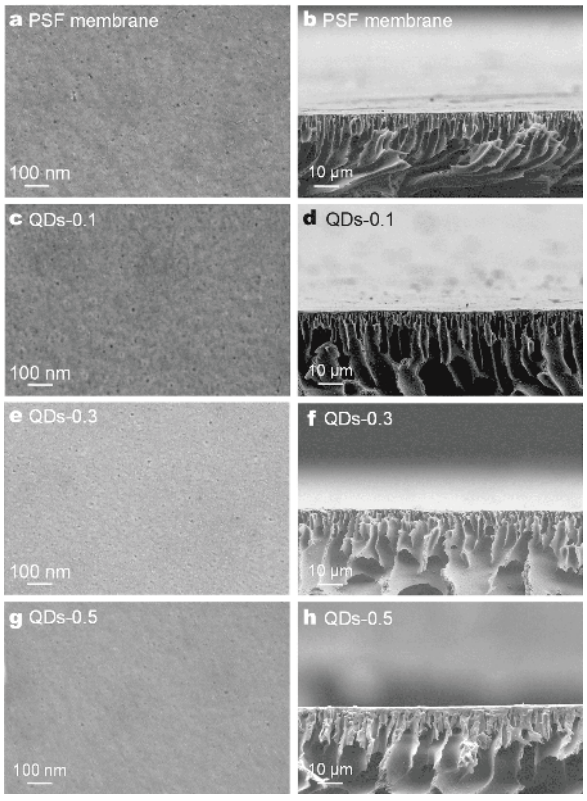

Figure 4 Surface and cross-sectional SEM images of the membranes: (a, b) PSF, (c, d) QDs-0.1, (e, f) QDs-0.3, and (g, h) QDs-0.5.

thermodynamic enhancement played the dominant role in affecting the membrane pore structure. With further increase of the percentage of GO QDs (0.5 wt.%), kinetic hindrance became the primary influential factor.

The surface roughness is an important factor affecting the membrane fouling resistance. Foulants tended to adsorb and accumulate in the valleys of rougher membrane surfaces, leading to a significant flux decrease. AFM images of the membrane surfaces (scanning area: 20 μm ×20 μm) are shown in Fig. 5. The surface of pristine PSF membranes is flat with a small R_a value, which agrees with the SEM surface characterizations. Introduction of GO QDs has no obvious influences on the surface roughness.

The overall porosity of the membranes was increased when smaller amounts of GO QDs (0.1 wt.% and 0.3 wt.%) were added, while decreased when 0.5 wt.% GO QDs were added, as displayed in Fig. 6a. The porosity of QDs-0.3 membranes is 85.9% while that of the pristine PSF membranes is only 55.7%. A small amount of hydrophilic GO QDs increased the mutual diffusion between NMP and water in the phase inversion process, leading to a more porous structure of the modified membranes. The decrease in membrane porosity is attributed to the significant increase in the viscosity of the casting solution. Membrane surface hydrophilicity played a major role in affecting the permeability and fouling behavior. The water layer formed on a hydrophilic membrane surface helped reduce the adsorption and accumulation of foulants, leading to better membrane antifouling performance. Static water contact angles of membrane surfaces were measured to characterize their hydrophilicity, as

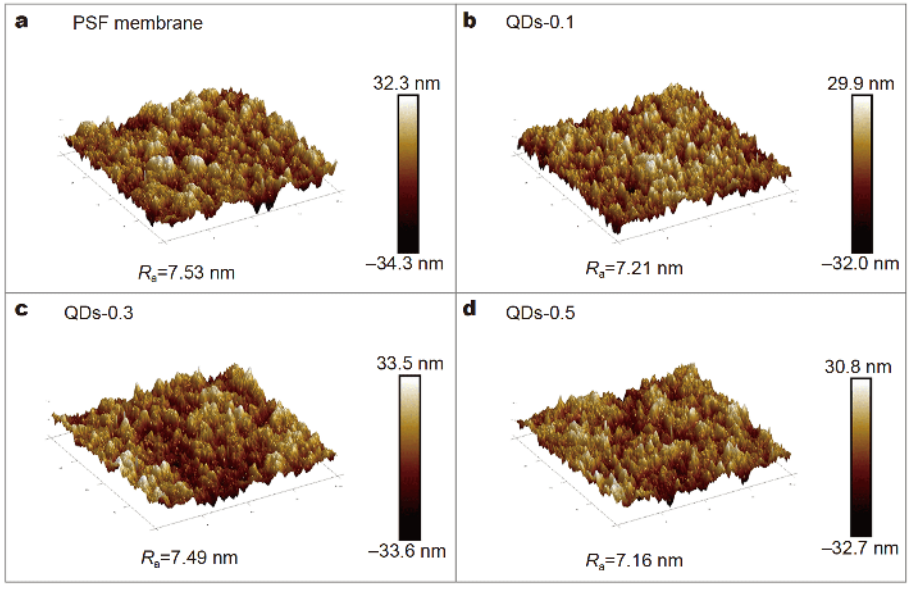

Figure 5 Three dimensional surface AFM images of the membranes: (a) PSF, (b) QDs-0.1, (c) QDs-0.3, and (d) QDs-0.5.

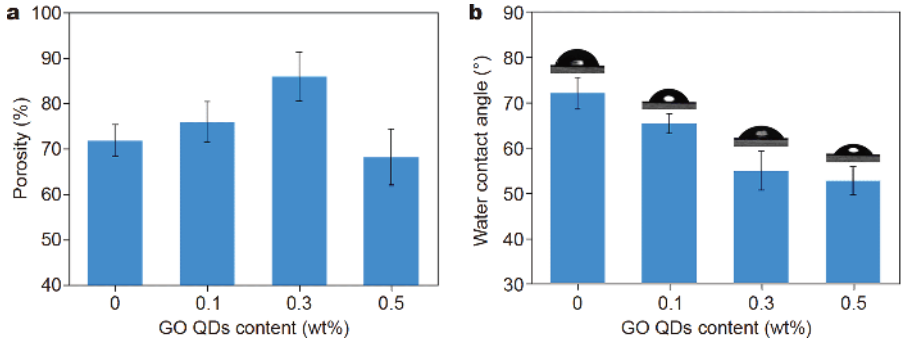

Figure 6 (a) Porosities and (b) water contact angles of the membranes with different GO QDs loading amounts.

shown in Fig. 6b. The pristine PSF membranes were inherently hydrophobic with a contact angle of 72.1°. As the content of GO QDs was increased from 0 to 0.5 wt.%, the hydrophilicity of the modified membrane was significantly improved. In the phase inversion process, GO QDs migrated to the membrane surfaces and pore walls spontaneously, leading to the increased membrane hydrophilicity. Comparing with GO sheets, the better dispersion of small sized GO QDs increased the amount of functional groups on the membrane surface.

Permeability and separation performance

The effects of GO QDs incorporation on membrane permeability and separation performance were investigated and the results are shown in Fig. 7. As can be seen from Fig. 7a, the pure water flux of pristine PSF membranes was 82.52 LMH bar^{-1}. The addition of GO QDs into PSF matrix led to a significant increase in membrane permeability, 108.69 LMH bar^{-1} for QDs-0.1 and 130.54 LMH bar^{-1} for QDs-0.3 membranes. When the loading of GO QDs was further increased to 0.5 wt.%, the permeability witnessed a decrease to 85.79 LMH bar^{-1}. The overall trend can be explained by the changes in membrane hydrophilicity and pore structure. The improved hydrophilicity helped attract more water molecules and facilitated their transport through the membranes. A more porous structure decreased the resistance to water transportation through creation of more space for water to flow. Comparing with pristine PSF, QDs-0.1 and QDs-0.3 membranes are more hydrophilic and porous, which accounts for the increased membrane permeability. However, a denser structure was formed for QDs-0.5 membranes, leading to the decrease in permeability.

The membrane flux of BSA solution showed a similar trend as pure water. It increased from 43.66 to 83.85 LMH bar^{-1} when the loading of GO QDs was increased from 0 to 0.3 wt.%. A higher loading of 0.5 wt.% led to a decrease in BSA flux to 56.86 LMH bar^{-1}. As shown in Fig. 7b, the rejection for BSA of pristine PSF was 100% and well maintained when GO QDs were incorporated. It is generally accepted that the rejection mechanism of UF membranes is sieving, which depends on the relative sizes of membrane pores and target solutes. The pore size was almost unchanged after incorporating GO QDs, which was confirmed by SEM characterizations. Furthermore, the strongly bound water molecules on the hydrophilic membrane surfaces helped

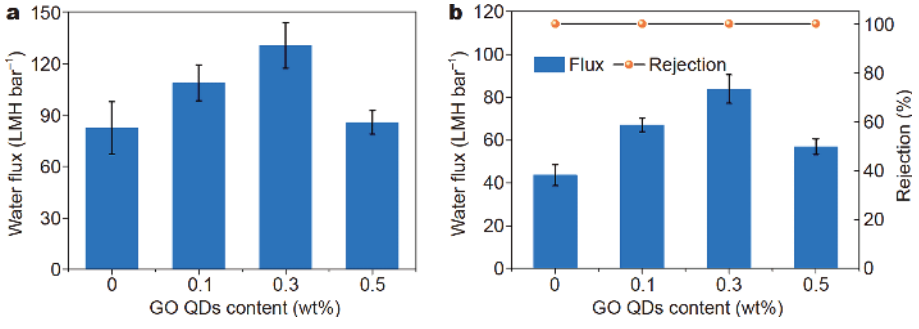

Figure 7 (a) Pure water flux of the membranes with different GO QDs loadings. (b) Membrane water flux in BSA solutions and their rejection performance. The tests were carried out in 500 ppm BSA solution in PBS under 0.1 MPa.

to prevent BSA from passing through the membranes.

Antifouling performance of the membranes

Fouling is an important limiting factor for UF membranes in practical applications, and leads to the decline of flux with time and the increase in operation costs. Proteins are often recognized as typical pollutants owing to their complex structure as well as their common existence in water. They frequently block membrane pores and adsorb onto membrane surfaces, leading to the increase in water transport resistance of the membranes. The antifouling performance of the prepared membranes was investigated in BSA aqueous solutions. Before measurements, all the membranes were pre-compacted under 0.2 MPa for 120 min to ensure that the flux decline was only caused by fouling. Membrane water flux as a function of time is displayed in Fig. 8a. There was a sharp decrease in water flux when the feed was switched from DI water to BSA solution for all the tested membranes. It can be seen from Fig. 8b that pristine PSF membranes experienced the most severe flux loss, up to 52.6%. The GO QDs incorporated membranes showed less water flux loss, indicating that they have better resistance to protein fouling. The pure water flux of all membranes could not be restored to the initial value by hydraulic cleaning, due to the difficulty of removing BSA molecules that strongly attached to the membrane surfaces and pore walls. However, the restoration rate of water flux was higher for GO QDs incorporated membranes, suggesting that the affinity of BSA molecules on pristine PSF was stronger, since they are both hydrophobic.

FRR is an important parameter when evaluating the antifouling performance of membranes. As seen from Fig. 8c, FRR of the membranes increased from 54.5% to 89.7% when the GO QDs loading was increased from 0 to 0.5 wt.%. BSA molecules are loosely attached to the membrane surfaces thus they can be removed by hydraulic washing. The improved antifouling performance of GO QDs modified membranes can be further demonstrated by R_{total}, R_r and R_{ir} of the membranes (Fig. 8d). Water flux decline caused by proteins is what we call the reversible fouling (R_r). Irreversible fouling (R_{ir}) results from the proteins that strongly attached to membrane surfaces or entered membrane pores. Pristine PSF membranes showed the highest R_{ir} of 33.3% due to the strong hydrophobic interactions between the membrane surface and BSA molecules. R_{ir} of the GO QDs modified membranes decreased significantly (21.2%, 15.1% and 10.3% for QDs-0.1, QDs-0.3 and QDs-0.5 membranes). The improved antifouling performance was attributed to the decreased affinity between BSA molecules and membrane surfaces.

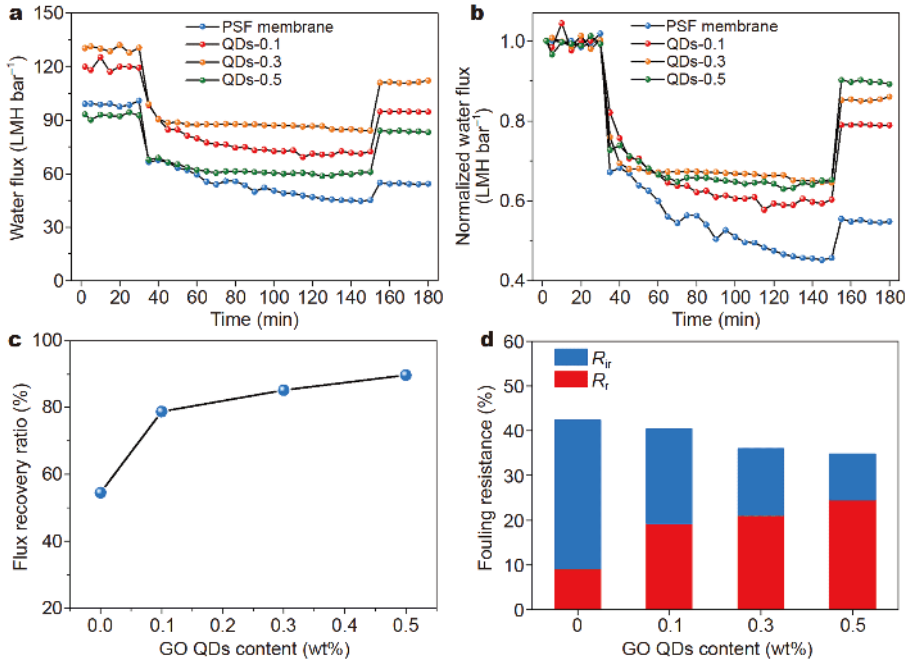

Figure 8 (a) Time-dependent water flux of the membranes with different GO QDs loadings. To make it clearer, the normalized membrane flux *versus* time is shown in (b). (c) Flux recovery ratio of the membranes. (d) Fouling resistance of the membranes.

Static BSA adsorption measurements

The cake layer formation governs the fouling process of UF membranes. The protein adsorption on the membrane surface is a direct and effective evidence to evaluate the antifouling performance. Static fluorescent BSA adsorption tests were conducted to investigate the effects of GO QDs incorporation on the protein adsorption amount. The membranes were immersed in fluorescent BSA solution with a concentration of 4 mg L^{-1} for 24 h and then photographed by CLSM (Fig. 9). As can be seen from Fig. 9a, BSA molecules tended to adsorb on the hydrophobic surface of pristine PSF membranes (bright green areas). Incorporating 0.1 wt.% GO QDs brought about a sharp decrease in the adsorption amount of BSA molecules on the modified membrane surfaces. When further increasing the loading of GO QDs, the amount of BSA adsorption continued to decrease but at a slower rate. This trend was the same as that of the membrane hydrophilicity. An aqueous layer was formed on the modified surfaces, which prevented the BSA molecules from contacting the membranes. As a result, the modified membranes with GO QDs had better ability to resist BSA adsorption comparing with pristine PSF membranes. The larger the amount of BSA adsorption is, the more severe the flux decline in the fouling process is, which was observed in the fouling measurements.

CONCLUSIONS

GO QDs, a novel kind of hydrophilic nanofiller, were incorporated into PSF UF membrane matrix during the phase inversion process to prepare nanocomposite membranes. The obtained membranes exhibited enhanced hydrophilicity, porosity, permeability and fouling resistance with a proper amount of GO QDs added. The enhanced membrane hydrophilicity was attributed to the rich functional groups of GO QDs that were exposed on the membrane surfaces and pore walls. The thermodynamic instability of the casting solutions caused by the incorporation of GO QDs accelerated the mass transfer between NMP and water during the phase inversion process, resulting in a more porous structure. The improved membrane hydrophilicity helped attract more

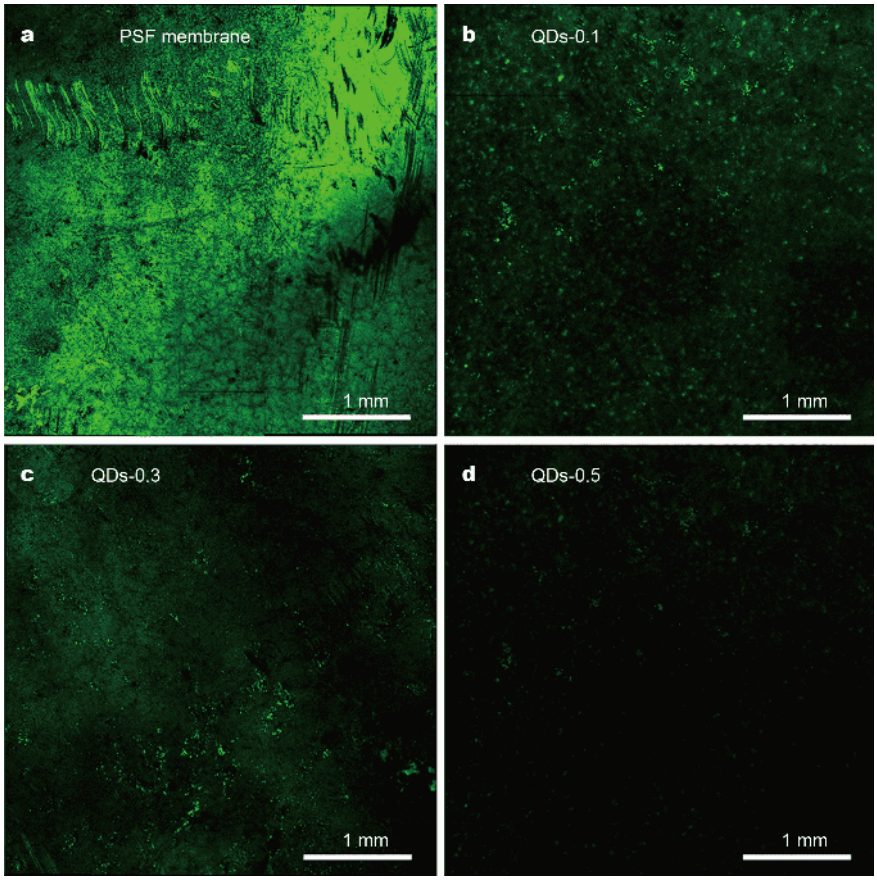

Figure 9 CLSM images of the membrane surfaces after static adsorption of FITC-BSA: (a) PSF, (b) QDs-0.1, (c) QDs-0.3, and (d) QDs-0.5.

water molecules and the porous structure facilitated their transport through the membranes, leading to an increased membrane permeability. The improved membrane hydrophilicity benefited its fouling resistance in two ways. Firstly, the hydration layer formed on the nanocomposite membrane surface prevented foulants from contacting the membranes directly. Secondly, the affinity between foulants and the hydrophilic membrane surfaces were reduced so that they could be easily removed by hydraulic cleaning. The results demonstrated that using GO QDs as nanofillers is an efficient way to prepare advanced UF membranes for water treatment.

Received 7 February 2019; accepted 15 March 2019; published online 29 March 2019

1 Shannon MA, Bohn PW, Elimelech M, *et al.* Science and technology for water purification in the coming decades. Nature, 2008, 452: 301–310
2 Oki T, Kanae S. Global hydrological cycles and world water resources. Science, 2006, 313: 1068–1072
3 Shaffer DL, Arias Chavez LH, Ben-Sasson M, *et al.* Desalination and reuse of high-salinity shale gas produced water: drivers, technologies, and future directions. Environ Sci Technol, 2013, 47: 9569–9583
4 Lee CW, Bae SD, Han SW, *et al.* Application of ultrafiltration hybrid membrane processes for reuse of secondary effluent. Desalination, 2007, 202: 239–246
5 Afonso MD, Bórquez R. Review of the treatment of seafood processing wastewaters and recovery of proteins therein by membrane separation processes—prospects of the ultrafiltration of wastewaters from the fish meal industry. Desalination, 2002, 142: 29–45
6 Chung YT, Mahmoudi E, Mohammad AW, *et al.* Development of polysulfone-nanohybrid membranes using ZnO-GO composite for enhanced antifouling and antibacterial control. Desalination, 2017, 402: 123–132
7 Gao W, Liang H, Ma J, *et al.* Membrane fouling control in ultrafiltration technology for drinking water production: A review. Desalination, 2011, 272: 1–8
8 Shi X, Tal G, Hankins NP, *et al.* Fouling and cleaning of ultrafiltration membranes: A review. J Water Process Eng, 2014, 1: 121–138
9 Otitoju TA, Ahmad AL, Ooi BS. Recent advances in hydrophilic modification and performance of polyethersulfone (PES) membrane*via* additive blending. RSC Adv, 2018, 8: 22710–22728
10 Chan R, Chen V. Characterization of protein fouling on membranes: opportunities and challenges. J Membrane Sci, 2004, 242: 169–188
11 Jhaveri JH, Murthy ZVP. A comprehensive review on anti-fouling nanocomposite membranes for pressure driven membrane separation processes. Desalination, 2016, 379: 137–154
12 Miller DJ, Dreyer DR, Bielawski CW, *et al.* Surface modification of water purification membranes. Angew Chem Int Ed, 2017, 56: 4662–4711
13 Grace JM, Gerenser LJ. Plasma treatment of polymers. J Dispersion Sci Tech, 2007, 24: 305–341
14 Wang H, Wang W, Wang L, *et al.* Enhancement of hydrophilicity and the resistance for irreversible fouling of polysulfone (PSF) membrane immobilized with graphene oxide (GO) through chloromethylated and quaternized reaction. Chem Eng J, 2018, 334: 2068–2078
15 Lee J, Chae HR, Won YJ, *et al.* Graphene oxide nanoplatelets composite membrane with hydrophilic and antifouling properties for wastewater treatment. J Membrane Sci, 2013, 448: 223–230
16 Kumar M, Gholamvand Z, Morrissey A, *et al.* Preparation and characterization of low fouling novel hybrid ultrafiltration membranes based on the blends of GO-TiO_2 nanocomposite and polysulfone for humic acid removal. J Membrane Sci, 2016, 506: 38–49
17 Wu H, Tang B, Wu P. Development of novel SiO_2-GO nanohybrid/polysulfone membrane with enhanced performance. J Membrane Sci, 2014, 451: 94–102
18 Yan L, Li Y, Xiang C, *et al.* Effect of nano-sized Al_2O_3-particle addition on PVDF ultrafiltration membrane performance. J Membrane Sci, 2006, 276: 162–167
19 Bottino A, Capannelli G, Comite A. Preparation and characterization of novel porous PVDF-ZrO_2 composite membranes. Desalination, 2002, 146: 35–40
20 Huang ZQ, Zheng F, Zhang Z, *et al.* The performance of the PVDF-Fe_3O_4 ultrafiltration membrane and the effect of a parallel magnetic field used during the membrane formation. Desalination, 2012, 292: 64–72
21 Ng LY, Mohammad AW, Leo CP, *et al.* Polymeric membranes incorporated with metal/metal oxide nanoparticles: A comprehensive review. Desalination, 2013, 308: 15–33
22 Sun P, Wang K, Zhu H. Recent developments in graphene-based membranes: structure, mass-transport mechanism and potential applications. Adv Mater, 2016, 28: 2287–2310
23 Huang H, Ying Y, Peng X. Graphene oxide nanosheet: an emerging star material for novel separation membranes. J Mater Chem A, 2014, 2: 13772–13782
24 Gopinadhan K, Hu S, Esfandiar A, *et al.* Complete steric exclusion of ions and proton transport through confined monolayer water. Science, 2019, 363: 145–148
25 You Y, Jin XH, Wen XY, *et al.* Application of graphene oxide membranes for removal of natural organic matter from water. Carbon, 2018, 129: 415–419
26 Nair RR, Wu HA, Jayaram PN, *et al.* Unimpeded permeation of water through helium-leak-tight graphene-based membranes. Science, 2012, 335: 442–444
27 Lian B, De Luca S, You Y, *et al.* Extraordinary water adsorption characteristics of graphene oxide. Chem Sci, 2018, 9: 5106–5111
28 Lv J, Zhang G, Zhang H, *et al.* Graphene oxide-cellulose nanocrystal (GO-CNC) composite functionalized PVDF membrane with improved antifouling performance in MBR: Behavior and mechanism. Chem Eng J, 2018, 352: 765–773
29 Hegab HM, Zou L. Graphene oxide-assisted membranes: Fabrication and potential applications in desalination and water purification. J Membrane Sci, 2015, 484: 95–106
30 Zhao G, Li X, Huang M, *et al.* The physics and chemistry of graphene-on-surfaces. Chem Soc Rev, 2017, 46: 4417–4449
31 Zhao H, Wu L, Zhou Z, *et al.* Improving the antifouling property of polysulfone ultrafiltration membrane by incorporation of isocyanate-treated graphene oxide. Phys Chem Chem Phys, 2013, 15: 9084–9092
32 Zambare RS, Dhopte KB, Patwardhan AV, *et al.* Polyamine functionalized graphene oxide polysulfone mixed matrix membranes

with improved hydrophilicity and anti-fouling properties. Desalination, 2017, 403: 24–35
33 Xu ZW, Zhang J, Shan M, *et al.* Organosilane-functionalized graphene oxide for enhanced antifouling and mechanical properties of polyvinylidene fluoride ultrafiltration membranes. J Membrane Sci, 2014, 458: 1–13
34 Safarpour M, Vatanpour V, Khataee A. Preparation and characterization of graphene oxide/TiO_2 blended PES nanofiltration membrane with improved antifouling and separation performance. Desalination, 2016, 393: 65–78
35 Zheng XT, Ananthanarayanan A, Luo KQ, *et al.* Glowing graphene quantum dots and carbon dots: properties, syntheses, and biological applications. Small, 2015, 11: 1620–1636
36 Li Y, Zhao Y, Cheng H, *et al.* Nitrogen-doped graphene quantum dots with oxygen-rich functional groups. J Am Chem Soc, 2012, 134: 15–18
37 Song X, Zhou Q, Zhang T, *et al.* Pressure-assisted preparation of graphene oxide quantum dot-incorporated reverse osmosis membranes: antifouling and chlorine resistance potentials. J Mater Chem A, 2016, 4: 16896–16905
38 Fathizadeh M, Tien HN, Khivantsev K, *et al.* Polyamide/nitrogen-doped graphene oxide quantum dots (N-GOQD) thin film nanocomposite reverse osmosis membranes for high flux desalination. Desalination, 2019, 451: 125–132
39 Bi R, Zhang Q, Zhang R, *et al.* Thin film nanocomposite membranes incorporated with graphene quantum dots for high flux and antifouling property. J Membrane Sci, 2018, 553: 17–24
40 Xu S, Li F, Su B, *et al.* Novel graphene quantum dots (GQDs)-incorporated thin film composite (TFC) membranes for forward osmosis (FO) desalination. Desalination, 2019, 451: 219–230
41 Wang M, Pan F, Yang L, *et al.* Graphene oxide quantum dots incorporated nanocomposite membranes with high water flux for pervaporative dehydration. J Membrane Sci, 2018, 563: 903–913
42 Wang H, Lu X, Lu X, *et al.* Improved surface hydrophilicity and antifouling property of polysulfone ultrafiltration membrane with poly(ethylene glycol) methyl ether methacrylate grafted graphene oxide nanofillers. Appl Surf Sci, 2017, 425: 603–613

Acknowledgements This work was supported by Beijing Natural Science Foundation (2172027).

Author contributions Zhu H supervised the project. Zhao G designed and performed the experiments. Hu R and Li J participated in interpreting and analyzing the data. Zhao G wrote the manuscript with support from Zhu H. All the authors commented on the manuscript.

Conflict of interest The authors declare no conflict of interest.

Supplementary information Supporting materials are available in the online version of this paper.

Guoke Zhao received her BSc degree from Northwestern Polytechnical University in 2016. She is currently a PhD candidate with Prof. Hongwei Zhu at the School of Materials Science and Engineering, Tsinghua University, China. Her current research focuses on graphene oxide based membranes for water treatment.

Hongwei Zhu is a Professor of the School of Materials Science and Engineering, Tsinghua University, China. He received his BSc degree in mechanical engineering (1998) and PhD degree in materials processing engineering (2003) from Tsinghua University. After postdoctoral research in Japan and USA, he began his independent career as a faculty member at Tsinghua University (2008-present). His current research interests involve structural design and engineering of nanomaterials for energy and environmental applications.

氧化石墨烯量子点改性聚砜超滤膜及其亲水性、水通量和抗污染性能研究

赵国珂, 胡蕊蕊, 李晶, 朱宏伟*

摘要 氧化石墨烯(GO)是一种有效的对高分子膜进行添加改性的亲水性纳米材料, 氧化石墨烯量子点(GO QDs)在保持GO结构的同时, 其小尺寸所致的边缘效应, 使其具有更加丰富的含氧官能团. 本文采用相转化法制备了GO QDs改性的聚砜超滤膜, 合适添加量的GO QDs提高了复合膜的孔隙率和亲水性. 当GO QDs添加量为0.3 wt.%时, 复合膜的水通量提高了60%(130.54 *vs.* 82.52 LMH bar^{-1}), 并实现了对牛血清白蛋白分子的完全截留. 在抗污染测试中, GO QDs添加量为0.5 wt.%的复合膜具有最高的通量回复率(89.7%)和最低的不可逆污染率(10.3%). 该研究表明GO QDs作为添加改性材料, 可有效提高聚砜超滤膜的亲水性、水通量和抗污染性能.

